The ISC Int'l Journal of Information Security

January 2011, Volume 3, Number 1 (pp. 51–66)
http://www.isecure-journal.org

Intelligent Scalable Image Watermarking Robust against Progressive DWT-Based Compression Using Genetic Algorithms

Mehran Deljavan Amiri [a,*], Habibollah Danyali [a,b], and Bahram Zahir-Azami [a,c]

[a] *Department of Electrical and Computer Engineering, University of Kurdistan, P.O. Box 416, Sanandaj, Iran.*
[b] *Department of Telecommunication Engineering, Shiraz University of Technology, P.O. Box 71555-313, Shiraz, Iran.*
[c] *Electrical and Computer Engineering Department, Ryerson University, Toronto, Ontario, Canada.*

ARTICLE INFO.

Article history:
Received: 22 September 2009
Revised: 24 August 2010
Accepted: 19 September 2010
Published Online: 17 January 2011

Keywords:
Image Watermarking, Genetic Algorithms, Intelligent, DWT, Scalability, Multiresolution, Robust, SPIHT

ABSTRACT

Image watermarking refers to the process of embedding an authentication message, called watermark, into the host image to uniquely identify the ownership. In this paper a novel, intelligent, scalable, robust wavelet-based watermarking approach is proposed. The proposed approach employs a genetic algorithm to find nearly optimal positions to insert watermark. The embedding positions coded as chromosomes and GA operators (e.g. selection, crossover, mutation and elitism), are used to find the nearly optimal embedding positions. A fitness function, which includes both factors related to transparency and robustness, is used to assess and compare chromosomes. The watermarked test images do not show any perceptual degradation. This approach supports scalable watermark detection and provides robustness against progressive wavelet image compression. The experimental results very efficiently prove the robustness of the approach against progressive wavelet image coding even at very low bit-rates and some other attacks. This approach is a good candidate for providing efficient authentication for secure and progressive image transmission applications especially over heterogeneous networks, such as the Internet.

1 Introduction

The rapid expansion and proliferation of the Internet, development of high capacity storage devices and the advances of data digitization in recent decades all have rapidly increased the availability and exchange of digital data to the public. These facts, combined with faster personal computers and powerful data processing software, required a reliable copyright protection system of multimedia data (e.g. audio, images, video) against unauthorized copy, illegal distribution and forgery. Of the many approaches existent to protect digital data, especially multimedia data, digital watermarking is probably the one that has received the most interest [1, 2]. Digital watermarking refers to the process of embedding an authentication message such as text, sound or a logo image, called watermark, into the digital data content which uniquely identifies the data ownership.

Depending on the problem that watermarking is being used to solve, a good watermarking system should satisfy some of the following requirements: transparency or fidelity, robustness, blindness, low false positive detection rate, security [1–9] and scalability [10, 11]. The transparency or fidelity means

* Corresponding author.
Email addresses: deljavan@ieee.org (M. Deljavan Amiri), hdanyali@ieee.org (H. Danyali), zahir@ieee.org (B. Zahir-Azami).
ISSN: 2008-2045

that the watermark insertion should not perceptually degrade the quality of the host image. Cox *et al.* [1] have defined transparency or fidelity as the perceptual similarity between the original and the watermarked versions of the cover work. Robustness implies that the watermark should be detectable from the watermarked data even after being attacked by common intentional or unintentional signal processing attacks. As a matter of fact, in a robust watermarking system, the watermark should withstand against common processing of the watermarked data such as lossy compression, spatial filtering, added noise, printing and re-scanning and geometric distortions (rotation, translation, scaling, and so on) as well. Blindness refers to the ability of detecting watermark in the absence of original host data. A false positive detection refers to the event that the watermark detector reports a watermark to be present in data in which the watermark in fact has not been embedded. In a good watermarking system, the rate of this mistake has to be extremely low. Security implies that the embedded watermark must not be easily detectable, maskable or removable by unauthorized users intended to thwart the watermarking purpose. Scalability in our context, refers to a potential in the watermarked data that allows reconstructing the lower resolutions of the watermark from the watermarked data. In a scalable watermarking system, even after applying an attack on the watermarked data which causes that the full resolution of the watermark may not be recoverable, it would be possible to at least reconstruct a lower resolution of the watermark.

Inserting a watermark into a host image can be performed in both spatial and frequency domains. The spatial domain image watermarking methods act directly on the host image pixels. Although the spatial watermarking methods are simple and easy to implement, they are weak against attacks and noise [1]. The frequency domain watermarking methods are performed on the coefficients of transformed image after applying a transform such as DCT (discrete cosine transform), DFT (discrete Fourier transform) or DWT (discrete wavelet transform) to the host image [6].

There have been some researches in application of genetic algorithms in image watermarking algorithms [12–17]. The proposed watermarking approach in [12] improves the performance of an existing algorithm [13] using genetic algorithms optimization. The watermarking system in [12] proposes an optimization process where a genetic algorithm searches for the optimum values of the parameters which improve the visual quality of the watermarked image and the robustness of the watermark. In [14], Aslantas has presented an optimal watermarking algorithm based on singular-value decomposition using genetic algorithms. In this algorithm, the singular values of the host image are modified by multiple scaling factors to embed the watermark image. Modifications are optimized using GA to obtain a high robustness for watermark without increasing the transparency of the host image. The watermarking algorithm described in [16] presents a robust technique for embedding the watermark of signature information or textual data around the region-of-interest of a medical image based on genetic algorithms. In [15], Ketcham *et al.* propose an intelligent watermarking scheme for audio signal based on genetic algorithms in the DWT domain which is robust against watermarking attacks. They employed genetic algorithms for the optimal localization and intensity of watermark. Lee *et al.* [17] have proposed a watermarking algorithm in the DWT domain using genetic algorithms. In this algorithm, the watermark insertion is done in the DWT domain and a genetic algorithm is being used to extract the watermark. This method is robust against various attacks such as JPEG image compression and geometric transformations. It can be deducted from the existing results in [12–17] that employing a GA to improve the performance of the existing watermarking algorithms was successful. Taking to account the fact that the GAs are powerful optimization tools [18, 19], the optimized factors in the proposed GA-based watermarking algorithms are commonly the transparency and the robustness of the algorithm and consequently the overall performance of the watermarking system.

One of the most important and the most commonly used processes on digital images is compression. In the recent decades, DWT-based image coding approach has been an important field of research [20]. Due to the inherent multiresolution signal representation by DWT, DWT-based coding systems have also the potential to support both SNR and spatial scalability [21, 22]. As a consequence, many DWT-based image coding approaches have been developed such as SPIHT [23] and JPEG2000 [24, 25]. These coding approaches provide higher compression rates with much better quality compared to DCT-based JPEG standard and support scalability and progressive lossy to lossless coding features which are among the important requirement features for the new generation of image coding.

Several researches on digital image watermarking compatible to wavelet-based image compression have been reported in the literature [10, 26–33]. These methods try to provide a robust watermarking system against wavelet-based compression. In [31] Zaid, *et al.* introduce a watermarking algorithm robust against lossy compression, by exploring the use of turbo trellis-coded quantization techniques on the wavelet domain. This scheme is robust against lossy wavelet-based com-

pression methods such as JPEG2000 and SPIHT. The proposed approach in [32] implements image watermarking in the domain of an overcomplete, or redundant wavelet transform and is robust against SPIHT algorithm. In [33] Makhloufi *et al.* attempt to integrate watermarking in wavelet-based image coding. In this approach the watermark embedding is directly performed on the wavelet coefficients before the quantization phase of the coding algorithm. The watermarking algorithm described in [26] first applies 3 levels of wavelet transform to the host image and then inserts the watermark data into the coefficients of the lowest frequency subband. In [27] a secret message is directly embedded in a SPIHT encoded bitstream. This process allows to reconstruct the secret message during the decoding process. The watermarking method proposed in [29] first decomposes the watermark into a pyramid of low resolution image and higher level differences and then adds the decomposed data into the DWT coefficients of the host image. The approach proposed in [30] first applies 4 levels of wavelet transform on the host image and then inserts the watermark data into the coefficients of the lowest frequency subband using a weighing function. This method provides robustness of watermark against wavelet based compression. Taking into account the robustness feature of these methods against wavelet based compressions, none of them supports any of SNR and spatial scalability (i.e. multiresolution detection) features for watermark detection.

In our previous work, we have proposed a scalable image watermarking algorithm [10] in the DWT domain which is robust against DWT-based image compression. Although that approach supports multiresolution detection for the watermark, one of its possible drawbacks is that there the watermark data are inserted into fixed positions. In this paper, we are going to increase the performance of that system [10] using genetic algorithms. The embedding positions are simulated as chromosomes in the evolution process. Then the nearly optimal embedding positions are obtained by evolution of chromosomes using natural selection and GA operators. Thus, the whole evolution of GA can efficiently achieve high quality watermarked image and highly robust image against DWT-based compression.

The rest of this paper is organized as follows. Section 2 discusses some useful related preliminaries. Section 3 gives an overview of the proposed watermarking system. In Section 4, watermark insertion and detection algorithms are presented. Section 5 presents some details about the simulation of the system and provides various experimental results for test of the proposed approach, and finally, Section 6 concludes the paper.

2 Preliminaries

2.1 Discrete Wavelet Transform on Images

Applying one level of 2D-DWT on a $M \times N$ pixels digital image decomposes it into one approximate subband (sub-image) and 3 detail $M/2 \times N/2$ subbands, namely a low frequency subband LL_1, a horizontal high frequency detail subband HL_1, a vertical high frequency detail subband LH_1 and a diagonal high frequency detail subband HH_1. The total number of coefficients in the four subbands is equal to the original number of pixels in the image, i.e. $M \times N$. The low frequency subband (LL_1) is a low resolution (coarse) version of the original image. Its statistical characteristic are similar to the original image and contain the main part of the image's energy. High frequency subbands stand for the edges and textures of the image. To apply other levels of wavelet transform on an image, the low frequency subband of the previous level is used. Figure 1 demonstrates the decomposed Boat image 512×512 pixels after applying five levels of wavelet transform by 9/7 [34] filterbanks.

Human visual system has different sensitivities to each of the frequency subbands. This characteristic of human visual system is very much similar to the multiresolution analysis of wavelet transform at some extend. Therefore, the digital watermarking technique based on discrete wavelet transform can make an efficient use of the basic characteristics of human visual system, and can meet transparency and robustness, two important requirements of digital watermarking systems, at the same time.

2.2 A Review on Genetic Algorithms

Genetic algorithms (GAs), which were introduced by John Holland in 1975 for the first time [18], are global search methods that are based on Darwin's "survival of the fittest" theory and simulate the natural biological evolution to solve optimization problems [18, 19]. In the GAs, any candidate solution is represented by an encoded string, called "chromosome". To compare chromosomes, a fitness function is used. The fitness function generates (calculates) a fitness value for each chromosome. To find a nearly optimum solution, an evolution process is performed on a population of chromosomes. The goal of evolution is to adjust the elements in the chromosome (genes) to minimize or maximize the fitness value of the chromosome. Figure 2 depicts the flowchart of a typical genetic algorithm.

According to Figure 2, the evolution process starts by random creation of a population of chromosomes as the initial population. At the next step, the fitness value of each chromosome is calculated using a pre-

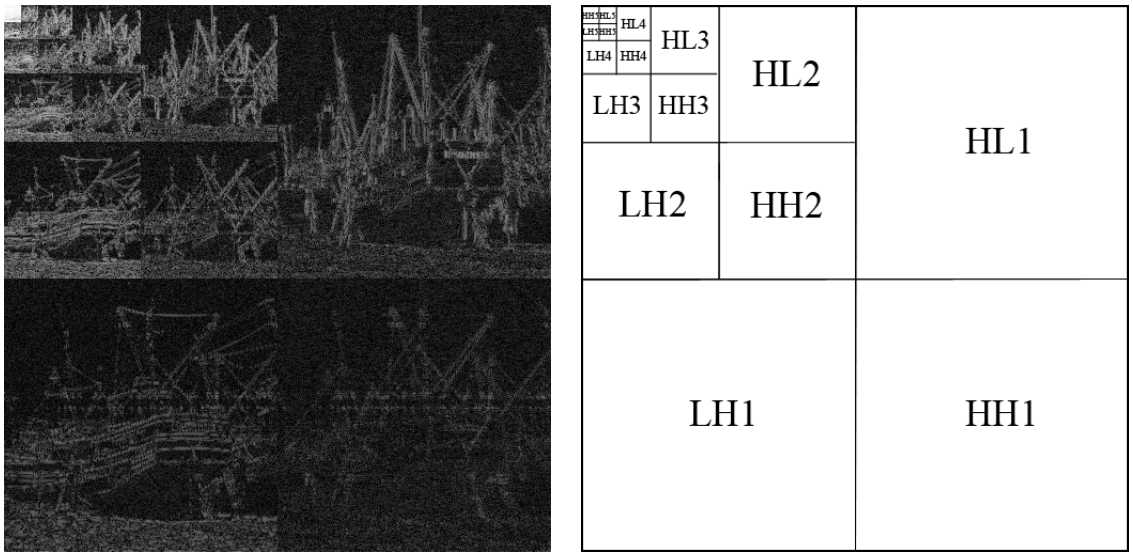

(a) Decomposed Boat after applying 5 Levels of 2D-DWT (scaled for better magnification of the differences).

(b) Conventional notation of (a).

Figure 1. Decomposition of Boat image.

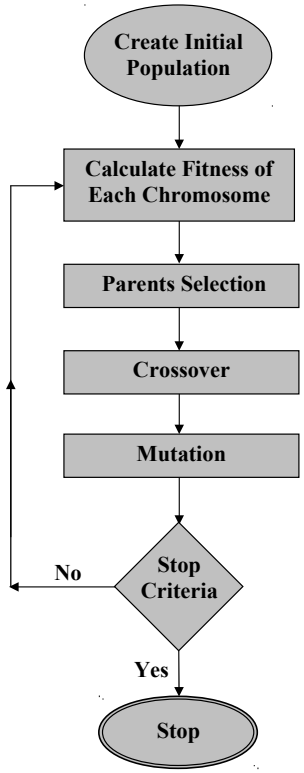

Figure 2. The flowchart of a typical GA.

defined fitness function. Then the chromosomes compete with each other to be selected as parents to produce offsprings. Fitter chromosomes have the greater chance to be selected and survive during the evolution process. The offsprings are then generated from the selected parents by using genetic operations, crossover and mutation. In crossover, a crossover point is selected between the first and last genes of the parents. Then, the fractions of two parents after the crossover point are exchanged, and two new offsprings are produced. In mutation, genes of the chromosomes are randomly changed based on predefined mutation rate. The process will repeat until a predefined condition is satisfied, or a constant number of iterations is reached.

2.3 Brief Review of Scalable Image Watermarking Approach

To insert watermark data into the host image, our previously proposed watermarking algorithm [10], first applies multi-level 2D-DWT to the host image to provide the wavelet coefficients pyramid. To have a multiresolution representation of the binary watermark, a multi level 2D down-sampling is applied to the watermark (see Figure 3(b)). Then the decomposed watermark subbands are inserted into the seven top subbands of the decomposed wavelet image as follows:

(a) 64 × 64 pixels watermark (logo) image.

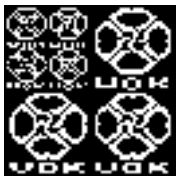

(b) Decomposed watermark after applying 2 levels of 2D down-sampling.

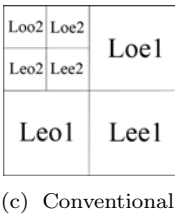

(c) Conventional notation of (b).

Figure 3. Multiresolution decomposition of a watermark.

Step 1: The coefficients (bits) of the subband Loo_2 are placed into the 5th bit of the coefficients of the subband LL_5.
Step 2: The coefficients of subbands Loe_2, Leo_2 and Lee_2 are placed into the 4th bit of the coefficients of subbands HL_5, LH_5 and HH_5, respectively.
Step 3: The coefficients of subbands Loe_1, Leo_1 and Lee_1 are placed into the 3rd bit of the coefficients of subbands HL_4, LH_4 and HH_4, respectively.

The watermarked DWT coefficients are then encoded by a DWT-based image compression algorithm such as SPIHT or HS-SPIHT, as a highly scalable modification of SPIHT, to provide an embedded progressive (by quality and/or resolution) bitstream. Before extracting watermark data, the encoded watermarked bitstream is first truncated at the decoder budget (bit-rate) and then decoded to reconstruct the watermarked DWT coefficients of the image. At the watermark extraction step, binary data of each of the multiresolution decomposed watermark subbands are extracted from the reconstructed watermarked DWT coefficients. Multiple spatial resolutions (e.g. quarter, half and full) of the watermark (see Figure 3) are then reconstructible from the extracted decomposed watermark data.

3 Overview of The Proposed GA-Based Scalable Watermarking System

This section illustrates our proposed intelligent image authentication approach. Our previous proposed scalable image watermarking system [10] embeds watermark data into fixed positions in the wavelet image. In this new work, we utilize a GA to find nearly optimal embedding positions in DWT subbands.

The proposed system is depicted in Figure 4. This procedure is performed for each chromosome of the population in all of the generations. On the insertion side a multi level 2D-DWT is applied to the host image to provide the wavelet coefficients pyramid. Figure 1 shows the decomposed Boat image after applying 5 levels of 2D-DWT and its conventional subband notation. A binary logo image is used as watermark (see Figure 3). A multiresolution decomposition of the watermark, is also provided by applying a multi level 2D down-sampling to the binary watermark. Figure 3(b) shows the multiresolution representation of the binary watermark after applying 2 levels of down-sampling, which results in 7 resolution subbands similar to a 2-level 2D-DWT decomposition. The decomposed watermark coefficients are then inserted into the 7 top subbands of the decomposed image according to the positions which are introduced by the chromosome (see Figure 5). The watermarked DWT coefficients are then encoded by a DWT-based image compression algorithm such as SPIHT or HS-SPIHT to provide an embedded progressive (by quality and/or resolution) bitstream. Also, to evaluate the transparency of the watermarked image, a multi level 2D-IDWT is applied to the watermarked coefficients which results the watermarked image. The fidelity of the watermarked image is measured by PSNR (peak signal-to-noise ratio).

On the watermark extraction side, the input bitstream is first truncated at the decoder budget (bit-rate) and then decoded to reconstruct the watermarked DWT coefficients of the image. By applying multi levels of 2D inverse DWT (2D-IDWT), the watermarked image for the decoder bit-rate rate is reconstructed. At the watermark extraction step, binary data of the multiresolution decomposed watermark is extracted from the reconstructed watermarked DWT coefficients. Multiple spatial resolution of the watermark is then reconstructible from the extracted decomposed watermark data. Watermark insertion and detection algorithms will be discussed in details in Section 4

According to the definition of GAs, we need to define a fitness function to evaluate chromosomes. The fitness value for each chromosome C in the proposed GA is defined as:

$$\mathrm{F_C} = \mathrm{PSNR_C} + \beta \cdot (\mathrm{DR_{f,C,0.5}} + \mathrm{DR_{f,C,0.125}} + \mathrm{DR_{f,C,0.0625}})$$

Where F_C is the fitness of C and PSNR_C is the PSNR of the watermarked image using C. The quality of the reconstructed binary watermark is measured by DR (Detector Response) which is defined as:

$$\mathrm{DR} = \frac{\text{number of true extracted coefficients}}{\text{total number of watermark coefficients}} - 0.5$$

If the DR is 0.5, the original and reconstructed watermarks are completely the same. However, a DR value of -0.5 indicates a complete absence of the watermark.

In the fitness calculation process, $\mathrm{DR}_{f,C,h}$ is the quality of the detected full resolution watermark at the bit-rate h for $h = \{0.5, 0.125 \text{ and } 0.0625\}$ which has been inserted using C. Finally, β is a weighting factor for the DRs.

To provide a visual sense of the fitness calculation process, this process is depicted in Figure 6. The encoded watermarked bitstream is truncated and decoded at bit-rates 0.5, 0.125, 0.0625 bpp and the watermark's data is extracted from each decoded image. In this process, the PSNR plays the role of transparency measure and DR values play the role of robustness measure. Because the PSNR values are dozens of times

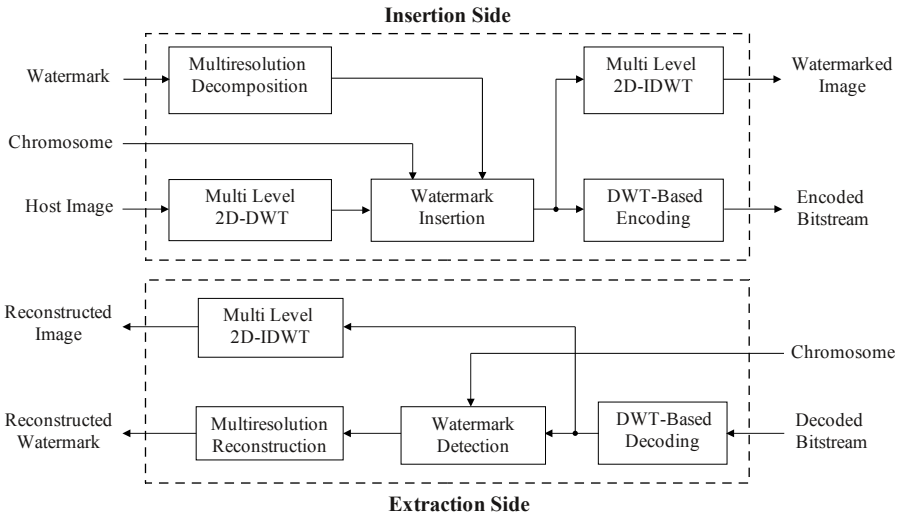

Figure 4. Block diagram of the proposed system.

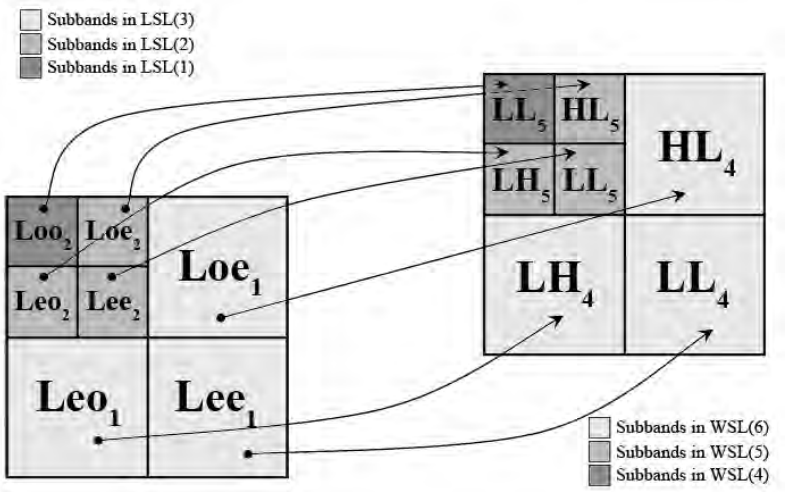

Figure 5. Corresponding subbands in the decomposed (down-sampled) watermark and the wavelet decomposed image.

larger than the associated DR values in the GA fitness function, there is a need to magnify the DR values with a weighting factor β to balance the influences caused by both the transparency and robustness requirements [35].

4 Chromosome Definition and Watermark Insertion and Detection Algorithms

4.1 Chromosome Definition

To use GAs as an optimization tool, first we need to define the structure of the chromosomes. The structure of the binary chromosomes is defined in a way that determines positions (a bit in each coefficient of seven top subbands in the wavelet pyramid) to insert the coefficients of the decomposed watermark (Figure 7). The first two genes of the chromosome in the Figure 7 (which are marked with (X_1,X_0)) are used to determine a position in the top-left coefficient of the lowest frequency subband of the wavelet image which the counterpart coefficient of the decomposed watermark will be placed on it. The position is determined by adding a constant value to the decimal value of the X_1X_0 (for example the decimal value for the X_1X_0= "10" is 2). Similar to the Top-left coefficient, to insert each coefficient of the decomposed watermark in to wavelet image, a position is determined by the chromosome.

4.2 Watermark Insertion Algorithm

Step 1: Apply 5 levels of 2D-DWT to the host image, I(x,y), to generate the wavelet image, W(x,y), which consists of one low frequency subband (LL_5) and 15

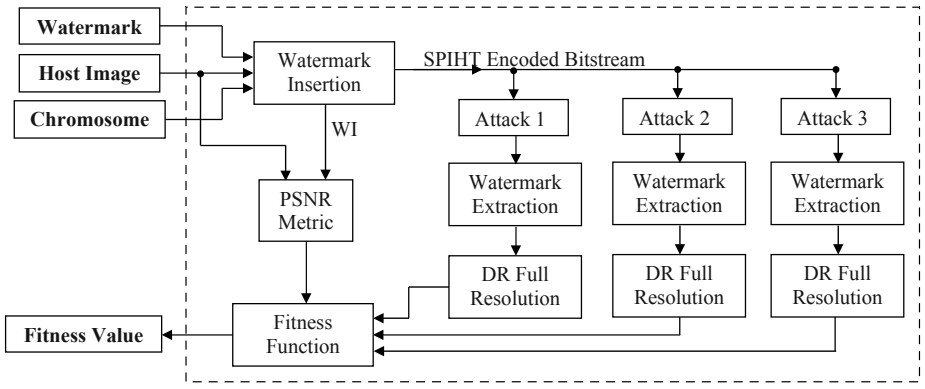

Attack 1: Decoding with 0.5 bpp
Attack 2: Decoding with 0.125 bpp
Attack 1: Decoding with 0.0625 bpp
WI: Watermarked Image

Figure 6. Block diagram of the fitness calculation process for each chromosome.

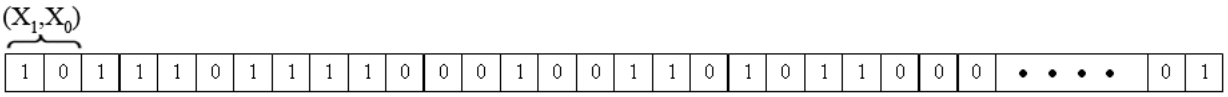

Figure 7. Sample chromosome definition (two times longer than the watermark size).

high frequency subbands (HL_i, LH_i, HH_i, for i=1 to 5) (see Figure 1). These subbands are classified according to their dependency to spatial resolution levels as follows:

- WSL(6) = $\{LL_5\}$
- WSL(i) = $\{HL_i, LH_i, HH_i\}$ for i=1 to 5
  WSL stands for Wavelet Subband Level.

Step 2: Apply 2 levels of 2D down-sampling to the binary watermark image, L(x,y), to generate 7 subbands, Loo_2 and Loe_j, Leo_j and Lee_j, j=1, 2 (see Figure 3). Also, these subbands are classified as follows:

- LSL(3) = $\{Loo_2\}$
- LSL(j) = $\{Loe_j, Leo_j, Lee_j\}$ for j=1, 2
  LSL stands for Logo Subband Level.

Step 3: for (i=1 to 3):
Insert LSL(i)'s subbands into WSL(i+3)'s subbands as follows:

- for each component (c) in the LSL(i)'s subbands and its corresponding coefficient (w) in its pair subband in the WSL(i+3):
  - assume X_1X_0 as the position introduced by chromosome for the c.
  - k = decimal (X_1X_0)
  - w $\gg$ (i+2+k)
  - Set LBS of w to 0
  - w $\ll$(i+2+k)
  - w = w + c $\times 2^{i+2+k}$

4.3 Watermark Detection Algorithm

Step 1: Apply 5 levels of 2D-DWT to the decoded watermarked image. The transformed image is named W_d(x,y) and the subbands in W_d(x,y) are classified in different subband levels (WSL_d(i)), in the same way as done in the insertion procedure.

Step 2: for (i=1 to 3):
extract LSL_d(i)'s subbands from WSL_d(i+3)'s subbands as follows:

- for each coefficient (w_d) in every subband of WSL_d(i+3):
  - assume X_1X_0 as the position introduced by chromosome for the c_d.
  - k_d = decimal(X_1X_0)
  - if (w_d mod 2^{i+3+k}) equals (w_d mod 2^{i+2+k}) then c_d=1 else c_d=0

Step 3:

- Take LSL_d(3) as the detected watermark at quarter resolution.
- Take LSL_d(3) and LSL_d(2) and apply one level reconstruction (i.e., inverse of the 2D down-sampling done in the insertion stage) to obtain detected watermark at half resolution.
- Take LSL_d(3), LSL_d(2) and LSL_d(1) and apply 2 levels of reconstruction to obtain detected watermark at full resolution.

One of the important notes about the proposed algorithm is the watermarking chromosome. After finishing the evolution process, the best chromosome (chromosome with the highest fitness value in the last

generation) is being selected as the watermarking chromosome. The chromosome contains a pair of binary numbers (X_1X_0) for each of the watermark coefficients. Therefore it's two times longer than the watermark, in size. For Example, if we use a 64×64 pixels binary image as watermark, the chromosome length will be 8192 bits ($2 \times 64 \times 64$). This bit string can be assumed as the watermarking key in the proposed system. Having a watermarking key in the watermarking algorithms could have positive and negative effects on the algorithm's application. The existence of the watermarking key increases security for watermark extraction and watermark can not be extracted by an adversary. On the other hand, the user needs to pay extra cost to carry or send the key to the extraction point and this might be pointed out as the major drawback of the proposed algorithm.

Table 1. Parameters setting for GA-based experiment.

Parameter	Value
Population size	20
Elitism rate	20%
Crossover rate	90%
Mutation rate	0.3%
Maximum number of generations	100
DR weighting factor (β)	40

5 Simulation Details and Experimental Results

The proposed system was fully software-implemented and has been tested on DWT-based image coding algorithms. For the following presented experiments, the standard images Boat and Gold-hill were used as test images. The size of these images is 512×512 pixels. The 9/7 taps filtering kernel [34] which is mainly used in the wavelet-based image compression literature has been used for computing the DWT. Table 1 shows the parameter settings to run the GA to find nearly optimal embedding positions. Figure 8 depicts the progress of the adaptation process to find the nearly optimal positions to insert watermark into Boat and Gold-hill images. As described in Section 3 the fitness value for each chromosome is composed of both transparency and robustness factors. Therefore, chromosomes with higher fitness warrant the transparency and robustness for the watermarked image. As Figure 8 shows, the average fitness of the population is in an increasing mode during the evolution process. This fact implies that the evolution process gradually discovers closer to optimal positions to insert the watermark data.

The following subsections describe the results of experiments carried out to test the various features of the proposed system and compare them with the results in our previous algorithm [10].

5.1 Transparency

To test the transparency of the proposed method both of Boat and Gold-hill images have been watermarked in two sets of independent experiments, once by our previous method [10] and once by the new proposed method. To measure the quality of the watermarked images, the PSNR (Peak Signal to Noise Ratio) and MSSIM (Mean Structural SIMilarity) indexes were used. The MSSIM index, which has been introduced by Wang *et al.* in [36, 37], is a human visual system-based index for measuring the similarity between two images and is suitable for watermarking researches. The maximum value for MSSIM index is 1 (when two images are completely equal) and its minimum value is 0. To aim a suitable transparency in image watermarking systems, the MSSIM value for the watermarked image should be close to 1.

The watermarked images using our previously proposed algorithm [10] are demonstrated in Figures 9(b), and 10(b) with PSNR 47.63 dB, MSSIM 0.918 and PSNR 45.89 dB, MSSIM 0.906. The GA-based algorithm gradually pushes the position of the solution towards the nearly optimal embedding positions and improves the quality of the watermarked image shown in Figures 9(c), and 9(d) and Figures 10(c), and 10(d). The quality of the watermarked images by the GA-based algorithm are much better than the watermarked images using previous algorithm and the quality is being improved when the number of generations increases.

5.2 Robustness against DWT-Based Compression and Multiresolution Watermark Detection

To test the scalability feature and robustness of the proposed watermarking approach against DWT-based image compression, a scenario of once encoding, multiple times decoding at various bit-rates (qualities) was used. A 64×64 pixels binary pseudo-random image was used as watermark. The watermarked wavelet coefficients of the test images were encoded by SPIHT. The encoder was set to support maximum required bit-rate. The encoded bitstreams were then decoded at various bit-rates (qualities) and 3 spatial resolutions (i.e., full, half and quarter) of the watermark were extracted at each bit-rate.

Table 2 shows the results obtained for multiresolution watermark detection from SPIHT compressed watermarked images for a wide range from very low bit-rate to high bit-rate. The results for our previous

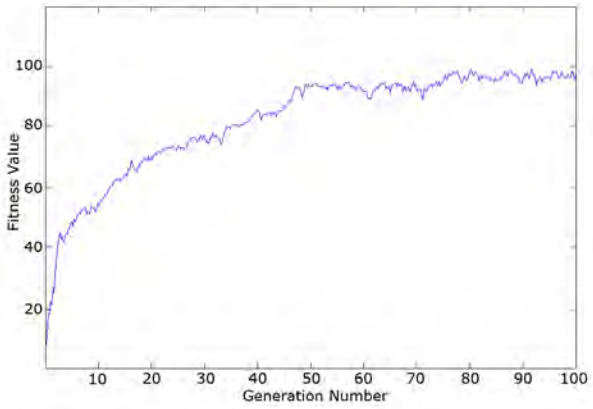

(a) Average fitness of the chromosomes under different GA generations to find nearly optimal positions in Boat.

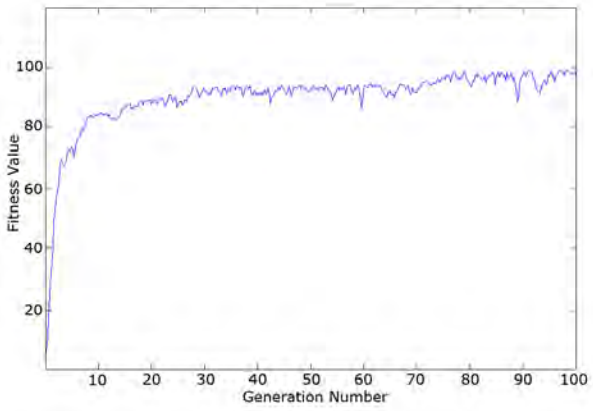

(b) Average fitness of the chromosomes under different GA generations to find nearly optimal positions in Gold-hill.

Figure 8. The progress of the adaptation process to find the nearly optimal positions to insert watermark.

algorithm [10] is also provided for comparison.

The results in Tables 2 and 3 indicate that the quarter resolution watermark is completely detectable at very low bit-rates (e.g. 0.1 bpp for Boat and 0.075 bpp for Gold-hill); whereas, the quarter resolution watermark in our previous algorithm [10] was detectable at 0.4 bpp and above for Boat image and 0.2 bpp and above for Gold-hill image. The half resolution watermark is fully reconstructible by spending more coding budget (e.g. at 0.2 bpp and above for both of Boat and Gold-hill images). With the previous algorithm, the half resolution watermark was detectable at 1 bpp for Boat and 0.4 bpp for Gold-hill. Finally, the full resolution watermark could be reconstructed at higher bit-rates (e.g. at 0.5 bpp and above for both images); whereas, in the previous algorithm it was detectable at 2 bpp and above for Boat and 1 bpp and above for Gold-hill. These results strongly prove that

Table 2. Results of multiresolution watermark detection for lossy decoding of the watermarked Boat images by SPIHT.

Bit-rate (bpp)	DR					
	GA-based algorithm			Previous algorithm		
	Quarter	Half	Full	Quarter	Half	Full
2	0.5	0.5	0.5	0.5	0.5	0.5
1	0.5	0.5	0.5	0.5	0.5	0.24
0.5	0.5	0.5	0.5	0.5	0.19	0.04
0.4	0.5	0.5	0.44	0.5	0.13	0.03
0.3	0.5	0.5	0.40	0.05	0	0
0.2	0.5	0.5	0.37	0.05	0	0
0.1	0.5	0.36	0.27	0	0	0
0.075	0.48	0.42	0.08	0	0	0
0.0625	0.29	0.09	0.04	0	0	0

Table 3. Results of multiresolution watermark detection for lossy decoding of the watermarked Gold-hill images by SPIHT.

Bit-rate (bpp)	DR					
	GA-based algorithm			Previous algorithm		
	Quarter	Half	Full	Quarter	Half	Full
2	0.5	0.5	0.5	0.5	0.5	0.5
1	0.5	0.5	0.5	0.5	0.5	0.5
0.5	0.5	0.5	0.5	0.5	0.5	0.26
0.4	0.5	0.5	0.45	0.5	0.5	0.18
0.3	0.5	0.5	0.44	0.5	0.23	0.05
0.2	0.5	0.5	0.40	0.5	0.20	0.04
0.1	0.5	0.41	0.24	0	0	0
0.075	0.5	0.29	0.10	0	0	0
0.0625	0.31	0.12	0.03	0	0	0

the proposed GA-based multiresolution watermarking approach is much more robust in dealing with the wavelet-based image compression methods and outperforms our previously proposed multiresolution watermarking algorithm [10].

5.3 Robustness against Scalable DWT-Based Compression

The proposed GA-based multiresolution watermarking approach was tested against scalable image coding. The watermarked Images were encoded by HS-SPIHT, a highly scalable modification of SPIHT [38, 39] which supports both SNR and spatial scalability for the encoded image. Tables 4 and 5 show the results for decoding the full spatial resolution (i.e. 512×512 pixels) of the watermarked images from the compressed bitstreams at various bit-rates. In Tables 6 and 7 similar results for decoding the compressed watermarked image at the quarter spatial resolution (i.e. 128×128 pixels) are shown. For both cases 3 resolutions of the wa-

(a) The original Boat image (512 × 512 pixels).

(b) The watermarked Boat using our previously proposed algorithm (PSNR is 47.63 dB and MSSIM is 0.918).

(c) The watermarked Boat using the best chromosome in the 70th generation (PSNR is 48.69 dB and MSSIM is 0.962).

(d) The watermarked Boat using the best chromosome in the 100th (last) generation (PSNR is 52.31 dB and MSSIM is 0.971).

Figure 9. Watermarking the Boat image using different algorithms and settings.

termark are extracted from the decoded watermarked images.

At the same bit-rate, the DR results in Tables 4 and 5 are much better than the counterpart results in Tables 6 and 7. The reason is that, when we target a lower spatial resolution, the coding budget that was spent for higher subbands coding at full resolution coding case, is now spent for the lower resolutions which contain watermark information. Therefore, more budget is spent for both lower resolution image and watermark as well and consequently the quality of the decoded watermarked image and the watermark in this case is better. By comparing the corresponding results in each row of Tables 4, 5, 6 and 7, it is clear that the robustness of the GA-based approach is much more than the previous approach. These results confirm that the use of GAs to find the nearly optimal positions to insert watermark, improves the robustness of the watermark against scalable DWT-based image compression.

Table 4. Results for lossy decoding of the compressed HS-SPIHT Boat bitstreams at full spatial resolution (512 × 512 pixels).

Bit-rate (bpp)	DR					
	GA-based algorithm			Previous algorithm		
	Quarter	Half	Full	Quarter	Half	Full
2	0.5	0.5	0.5	0.5	0.5	0.5
1	0.5	0.5	0.5	0.5	0.5	0.19
0.5	0.5	0.5	0.5	0.5	0.14	0.02
0.4	0.5	0.5	0.42	0.5	0.10	0.02
0.3	0.5	0.5	0.39	0	0	0
0.2	0.5	0.5	0.37	0	0	0
0.1	0.5	0.40	0.23	0	0	0
0.075	0.48	0.31	0.10	0	0	0
0.0625	0.26	0.09	0.06	0	0	0

(a) The original Gold-hill image (512 × 512 pixels).

(b) The watermarked Gold-hill using our previously proposed algorithm (PSNR is 45.89 dB and MSSIM is 0.906).

(c) The watermarked Gold-hill using the best chromosome in the 70th generation (PSNR is 47.91 dB and MSSIM is 0.951).

(d) The watermarked Gold-hill using the best chromosome in the 100th (last) generation (PSNR is 49.72 dB and MSSIM is 0.961).

Figure 10. Watermarking the Gold-hill image using different algorithms and settings.

Table 5. Results for lossy decoding of the compressed HS-SPIHT Gold-hill bitstreams at full spatial resolution (512 × 512 pixels).

Bit-rate (bpp)	DR					
	GA-based algorithm			Previous algorithm		
	Quarter	Half	Full	Quarter	Half	Full
2	0.5	0.5	0.5	0.5	0.5	0.5
1	0.5	0.5	0.5	0.5	0.5	0.5
0.5	0.5	0.5	0.5	0.5	0.5	0.5
0.4	0.5	0.5	0.45	0.5	0.5	0.19
0.3	0.5	0.5	0.39	0.5	0.5	0.13
0.2	0.5	0.5	0.37	0.5	0.20	0.05
0.1	0.5	0.40	0.23	0	0	0
0.075	0.5	0.31	0.10	0	0	0
0.0625	0.29	0.10	0.03	0	0	0

Table 6. Results for lossy decoding of the compressed HS-SPIHT Boat bitstreams at quarter spatial resolution (128 × 128 pixels).

Bit-rate (bpp)	DR					
	GA-based algorithm			Previous algorithm		
	Quarter	Half	Full	Quarter	Half	Full
0.5	0.5	0.5	0.5	0.5	0.5	0.5
0.4	0.5	0.5	0.5	0.5	0.5	0.5
0.3	0.5	0.5	0.49	0.5	0.5	0.44
0.2	0.5	0.5	0.41	0.5	0.43	0.11
0.1	0.5	0.48	0.31	0.22	0.10	0.04
0.075	0.5	0.30	0.18	0	0	0
0.0625	0.5	0.21	0.09	0	0	0
0.05	0.45	0.10	0.06	0	0	0

5.4 Robustness against Other Attacks

The robustness of the proposed scalable image watermarking algorithm is also tested against some attacks

Table 7. Results for lossy decoding of the compressed HS-SPIHT Gold-hill bitstreams at quarter spatial resolution (128 × 128 pixels).

Bit-rate (bpp)	DR					
	GA-based algorithm			Previous algorithm		
	Quarter	Half	Full	Quarter	Half	Full
0.5	0.5	0.5	0.5	0.5	0.5	0.5
0.4	0.5	0.5	0.5	0.5	0.5	0.5
0.3	0.5	0.5	0.5	0.5	0.5	0.5
0.2	0.5	0.5	0.44	0.5	0.5	0.21
0.1	0.5	0.5	0.37	0.5	0.20	0.11
0.075	0.5	0.38	0.21	0.06	0.01	0
0.0625	0.5	0.25	0.11	0	0	0
0.05	0.5	0.17	0.07	0	0	0

(other than compression), including two models of median filtering (using 3 × 3 and 5 × 5 window sizes), Gaussian filtering (mean = 0 and variance = 0.001), adding salt and pepper noise (on and off pixels ratio = 0.01) and cropping 25 percent of image's center (see Figures 11 and 12). Similar to the previous experiments, a 64 × 64 pixels binary pseudo-random image was used as watermark here. The watermarked Boat and Gold-hill images were attacked and the watermark was extracted from attacked images in different resolutions.

Table 8 shows the results obtained by this experiment. The results clearly show that the proposed approach is robust against the attacks. According to this table, in each row, the quality of the quarter resolution watermark is the maximum value in the DRs and the minimum value is for the full resolution watermark. This results clarify the multiresolution watermarking potential in the proposed algorithm again.

5.5 Comparisons with Other Wavelet-Based Algorithms

To give a final assessment of the validity of our new watermarking algorithm, some comparisons were performed with some state-of-the-art algorithms operating in the wavelet domain. Since the main novelty of our approach resides in the using GAs to increase the transparency and robustness of our scalable watermarking system against DWT-based image compression algorithms, we compare our results with the results in the papers which have introduced robust watermarking algorithms against DWT-based image compression. In this section, the results of the proposed algorithm are compared to the results obtained by the algorithms proposed in [26, 30, 31].

To compare the algorithms, the Boat and Gold-hill images were watermarked with the algorithms using a 64 × 64 pixels binary pseudo-random generated watermark. Table 9 compares the transparency results of the proposed GA-based algorithm with some state-of-the-art watermarking algorithms.

Table 8. Robustness of the watermark against some attacks (other that compression).

Image	Attack type	DR		
		Quarter	Half	Full
Boat	Median (3 × 3) filtering	0.46	0.46	0.42
	Median (5 × 5) filtering	0.41	0.37	0.34
	Gaussian noise	0.5	0.49	0.47
	Salt and pepper noise	0.41	0.37	0.37
	Cropping center	0.39	0.36	0.36
Gold-hill	Median (3 × 3) filtering	0.49	0.47	0.42
	Median (5 × 5) filtering	0.44	0.39	0.35
	Gaussian noise	0.5	0.5	0.48
	Salt and pepper noise	0.47	0.42	0.41
	Cropping center	0.39	0.36	0.35

To compare robustness of the algorithms, the watermarked images were encoded by SPIHT. The encoder was set to support the maximum required bit-rate. The encoded bitstreams were then decoded at various bit-rates (qualities) and the watermark was extracted from the decoded images. Taking into account the fact that none of the algorithms in [26, 30, 31] supports scalability for watermark extraction (the algorithms only detect a full resolution watermark), in this section, only the full resolution extracted watermark of the proposed algorithm is compared to the other algorithms' results.

Tables 10 and 11 show the results of detecting watermark from watermarked images using our algorithm and state-of-the-art algorithms with various bit-rates.

The results in Tables 9, 10 and 11 clearly demonstrate that the overall performance of the proposed GA-based approach is better than the other state-of-the-art algorithms. This improvement is the result of using GAs to find the nearly optimal positions to insert watermark to reach higher transparency and robustness.

6 Conclusions

An intelligent, scalable, robust and blind watermarking approach for scalable wavelet-based image compression was introduced. A multiresolution decomposition of the binary watermark image was performed by applying 2 levels of 2D down-sampling. The decomposed watermark subbands were inserted into their counterpart subbands of the wavelet decomposed im-

(a) 3×3 median filtering.

(b) 5×5 median filtering.

(c) Gaussian filtering.

(d) Salt and pepper noise.

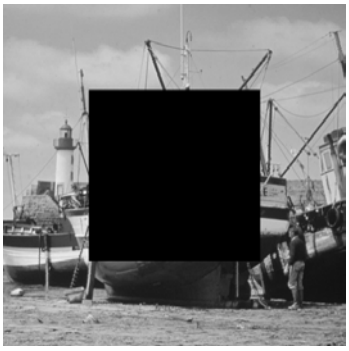

(e) Cropping 25 percent of image's center.

Figure 11. Attacked watermarked Boat image using different filterings.

(a) 3×3 median filtering.

(b) 5×5 median filtering.

(c) Gaussian filtering.

(d) Salt and pepper noise.

(e) Cropping 25 percent of image's center.

Figure 12. Attacked watermarked Gold-hill image using different filterings.

Table 9. Transparency comparison of the proposed algorithm against the other state-of-the-art algorithms.

Image	PSNR (dB)				MSSIM			
	The proposed algorithm	[31]	[26]	[30]	The proposed algorithm	[31]	[26]	[30]
Boat	52.31	42.06	37.41	41.63	0.971	0.926	0.874	0.943
Gold-hill	49.72	38.27	35.76	42.11	0.961	0.911	0.857	0.946

Table 10. Results for detecting watermark from watermarked Boat image.

Bit-rate (bpp)	DR			
	The proposed algorithm	[31]	[26]	[30]
2	0.5	0.5	0.5	0.5
1	0.5	0.5	0.5	0.5
0.5	0.5	0.48	0.5	0.44
0.4	0.44	0.41	0.14	0.36
0.3	0.40	0.33	0	0.32
0.2	0.37	0.21	0	0.23
0.1	0.27	0.05	0	0
0.075	0.08	0.05	0	0
0.0625	0.04	0.05	0	0

Table 11. Results for detecting watermark from watermarked Gold-hill image.

Bit-rate (bpp)	DR			
	The proposed algorithm	[31]	[26]	[30]
2	0.5	0.5	0.5	0.5
1	0.5	0.5	0.5	0.5
0.5	0.5	0.5	0.5	0.48
0.4	0.45	0.47	0.39	0.41
0.3	0.44	0.39	0.14	0.37
0.2	0.40	0.28	0	0.33
0.1	0.24	0.13	0	0.20
0.075	0.10	0	0	0.09
0.0625	0.03	0	0	0

age. A GA was used to find the nearly optimal positions to insert watermark into the coefficients of the wavelet pyramid. The embedding positions were coded as GA chromosomes and the GA operators were used to evolve a population of chromosomes. The PSNR results obtained for test images proved the transparency of the approach. The scalability feature and robustness of the proposed approach against DWT-based image compression, was evaluated by lossy compression of the watermarked image by the SPIHT algorithm. The compressed bitstream was decoded at different bit-rates. While at high bit-rates, full resolution watermark was completely detectable, at very low bit rates (e.g., 0.1 and 0.075 bpp) still a lower resolution of the watermark was preserved, which could authenticate the host image. To test the robustness of the proposed method against scalable DWT-based compression, the watermarked image was encoded by HS-SPIHT and decoded at different qualities and spatial resolutions. The results showed that at the same bit-rate, the qualities of the detected watermarks from decoded image at quarter spatial resolution are much better than the qualities of detected watermarks from decoded image at full spatial resolution. Inserting watermark into nearly optimal positions, high transparency and robustness against DWT-based image compression in conjunction with multiresolution watermark detection feature, make it attractive for secure image transmission applications especially over heterogeneous networks where different qualities of services need to be provided for end users.

References

[1] I.J. Cox, M.L. Miller, J.A. Bloom, J. Fridrich, and T. Kalker. *Digital Watermarking and Steganography*. Morgan Kaufmann, 2nd edition, 2008.

[2] I.J. Cox and M.L. Miller. A Review of Watermarking and the Importance of Perceptual Modeling. In *Proceedings of the International Conference on Electronic Imaging (SPIE'97)*, San Jose, CA, USA, 1997.

[3] N. Cvejic. *Algorithms for Audio Watermarking and Steganography*. PhD thesis, University of Oulu, Oulu, Finland, 2004.

[4] F. Hartung and M. Kutter. Multimedia Watermarking Techniques. *Proceedings of the IEEE*, 87 (7):1079–1107, 1999.

[5] G.C. Langelaar, I. Setyawan, and R.L. Lagendijk. Watermarking Digital Image and Video Data. A State-of-the-Art Overview. *IEEE Signal Processing Magazine*, 17:20–46, 2000.

[6] V.M. Potdar, S. Han, and E. Chang. A Survey of Digital Image Watermarking Techniques. In *Proceedings of the 3rd IEEE International Conference on Industrial Informatics (INDIN'05)*, pages 709–716, Perth, Australia, August 2005.

[7] C. Shoemaker. Hidden Bits: A Survey of Techniques for Digital Watermarking, Spring 2002. Available at http://web.vu.union.edu/~shoemakc/watermarking/watermarking.html.

[8] I.J. Cox and M.L. Miller. The First 50 Years of

Electronic Watermarking. *EURASIP Journal on Applied Signal Processing*, 2002(2):126–132, 2002.

[9] S. Craver, N. Memon, B. Yeo, and M. Yeung. Resolving Rightful Ownerships with Invisible Watermarking Techniques Limitations, Attacks, and Implications. *IEEE Journal on Selected Areas in Communications*, 16:573–586, may 1998.

[10] H. Danyali and M. Deljavan Amiri. A Mltiresolution Robust Watermarking Approach for Scalable Wavelet Image Compression. In *Proceedings of the 11th International Conference on Advanced Concepts for Intelligent Vision Systems (ACIVS'08)*, volume 5259 of *Lecture Notes in Computer Science*, pages 57–66, Juan-les-Pins, France, October 2008. Springer-Verlag Berlin Heidelberg.

[11] H. Danyali and M. Deljavan Amiri. A Scalable Blind Watermarking for Progressive Image Transmission. In *Proceedings of the 5th Iranian Conference on Machine Vision and Image Processing*, Tabriz, Iran, 2008.

[12] P. Kumsawat, K. Attakitmongcol, and A. Srikaew. A New Approach for Optimization in Image Watermarking by Using Genetic Algorithms. *IEEE Transactions on Signal Processing*, 53(12):4707–4719, dec. 2005.

[13] R. Dugad, K. Ratakonda, and N. Ahuja. A New Wavelet-Based Scheme for Watermarking Images. In *Proceedings of the 1998 IEEE International Conference on Image Processing (ICIP'98)*, volume 2, pages 419–423, Chicago, Illinois, USA, oct. 1998.

[14] V. Aslantas. A Singular-Value Decomposition-Based Image Watermarking Using Genetic Algorithm. *AEU - International Journal of Electronics and Communications*, 62(5):386–394, may 2008.

[15] M. Ketcham and S. Vongpradhip. Intelligent Audio Watermarking Using Genetic Algorithm in DWT Domain. *International Journal Of Intelligent Technology*, 2(2):135–140, 2007.

[16] F.Y. Shih and Y. Wu. Robust Watermarking and Compression for Medical Images Based on Genetic Algorithms. *International Journal of Information Sciences*, 175(3):200–216, October 2005.

[17] D. Lee, T. Kim, S. Lee, and J. Paik. Genetic Algorithm-Based Watermarking in Discrete Wavelet Transform Domain. In *Proceedings of the International Conference on Intelligent Computing (ICIC'06)*, volume 4113 of *Lecture Notes in Computer Science*, pages 709–716, Kunming, China, 2006.

[18] J.H. Holland. *Adaptation in Natural and Artificial Systems*. University of Michigan Press, Ann Arbor, MI, USA, 1975.

[19] D.E. Goldberg. *Genetic Algorithms in Search, Optimization and Machine Learning*. Addison-Wesley, Reading, Massachusetts, USA, 1989.

[20] N.J. Jayant, J. Johnson, and R. Safranek. Signal Compression Based on Models of the Human Perception. *Proceedgins of the IEEE*, 81(10):1385–1422, 1993.

[21] Y.K. Chee. Survey of Progressive Image Transmission Methods. *International Journal on Imaging Systems and Technology*, 10:3–19, 1999.

[22] J.M. Shapiro. Embeded Image Coding Using Zerotree of Wavelet Coefficients. *IEEE Transactions on Signal Processing*, 41(12):3445–3462, 1993.

[23] A. Said and W.A. Pearlman. A New, Fast, and Efficient Image Codec Based on Set Partitioning in Hierarchical Trees. *IEEE Transactions on Circuits and Systems for Video Technology*, 6(3): 243–250, June 1996.

[24] M. Charrier, D.S. Cruz, and M. Larsson. JPEG2000, the Next Mmillenium Compression Standard for Still Images. In *Proceedings of the 1999 IEEE International Conference on Multimedia Computing and Systems (ICMCS'99)*, pages 131–132, Florence, Italy, 1999.

[25] B.G. Haskell, P.G. Howard, Y.A. LeCun, A. Puria, J. Ostermann, M.R. Civanlar, L. Rabiner, L. Bottou, and P. Haffner. Image and Video Coding-Emerging Standards and Beyond. *IEEE Transactions on Circuits and Systems for Video Technology*, 8(7):814–837, 1998.

[26] D. Lee, T. Kim, S. Lee, and J. Paik. A Robust Watermarking Algorithm Using Attack Pattern Analysis. In *Proceedings of the 8th International Conference on Advanced Concepts for Intelligent Vision Systems (ACIVS'06)*, volume 4179 of *Lecture Notes in Computer Science*, pages 757–766, Antwerp, Belgium, September 2006.

[27] P. Tsai, Y. Hu, and C. Chang. A Progressive Secret Reveal System Based on SPIHT Image Transmission. *Signal Processing: Image Communication*, 19(3):285–297, 2004.

[28] P. Tsai, Y. Hu, and C. Chang. Using Set Partitioning in Hierarchical Trees to Authenticate Digital Images. *Signal Processing: Image communication*, 18(9):813–822, 2003.

[29] S.A.R. Jafri and S. Baqai. Robust Digital Watermarking for Wavelet-Based Compression. In *IEEE 9th Workshop on Multimedia Signal Processing (MMSP'07)*, pages 377–380, Chania, Crete, Greece, October 2007.

[30] M. Barni, F. Bartolini, and A. Piva. Improved Wavelet-Based Watermarking through Pixel-wise Masking. *IEEE Transactions on Image Processing*, 10:783–791, 2001.

[31] A.Q. Zaid, A. Makhloufi, and A. Bouallegue. Wavelet Domain Watermark Embedding Strategy Using TTCQ Quantization. *International*

Journal of Computer Science and Network Security (IJCSNS), 7(6):165–170, june 2007.

[32] K.M. Parker and J.E. Fowler. Redundant-Wavelet Watermarking with Pixel-wise Masking. In *Proceedings of the IEEE International Conference on Image Processing (ICIP'05)*, volume 1, pages 685–688, Genova, Italy, 2005.

[33] A. Makhloufi, A.Q. Zaid, R. Bouallegue, and A. Bouallegue. Watermark Integration to Wavelet Image Coding Scheme. In *Proceedings of the 8th IEEE International Symposium on Multimedia (ISM'06)*, pages 685–689, San Diego, CA, USA, 2006.

[34] M. Antonini, M. Barlaud, P. Mathieu, and I. Daubechies. Image Coding Using Wavelet Transform. *IEEE Transactions on Image Processing*, 1:205–220, 1992.

[35] M. Gen and R. Cheng. *Genetic Algorithms and Engineering Design*. Wiley, New York, NY, USA, 1997.

[36] Z. Wang, A.C. Bovik, H.R. Sheikh, and E.P. Simoncelli. Image Quality Assessment: From Error Visibility to Structural Similarity. *IEEE Transactions on Image Processing*, 13(4):600–612, Apr. 2004.

[37] Z. Wang, A.C. Bovik, H.R. Sheikh, and E.P. Simoncelli. The SSIM Index for Image Quality Assessment, Nov. 2010. Available at http://www.ece.uwaterloo.ca/~z70wang/research/ssim/.

[38] H. Danyali and A. Mertins. Highly Scalable Image Compression Based on SPIHT for Network Applications. In *Proceedings of the 2002 IEEE International Conference on Image Processing (ICIP'02)*, volume 1, pages 217–220, Rochester, NY, USA, 2002.

[39] H. Danyali and A. Mertins. Flexible, Highly Scalable, Object-Based Wavelet Image Compression Algorithm for Network Applications. *Vision, Image and Signal Processing, IEE Proceedings*, 151 (6):498–510, 2004.

Mehran Deljavan Amiri received his B.Sc. and M.Sc. degrees in Computer Engineering respectively from Islamic Azad University of Tabriz, Tabriz, Iran, in 2007 and University of Kurdistan, Sanandaj, Iran, in 2009. He worked as a research assistant and lecturer from 2008 to 2009 in the University of Kurdistan. As of April 2009, he is working as a technical analyser and programmer of auto-trading systems in the financial markets. He has published several technical papers. His research interests include artificial intelligent, steganography and watermarking, biometrics, image compression and auto-trading systems in the financial markets.

Habibollah Danyali received his B.Sc. and M.Sc. degrees in Electrical Engineering respectively from Isfahan University of Technology, Isfahan, Iran, in 1991 and Tarbiat Modarres University, Tehran, Iran, in 1993. From 1994 to 2000 he was with the Department of Electrical Engineering, University of Kurdistan, Sanandaj, Iran, as a lecturer. In 2004 he received his PhD degree in Computer Engineering from University of Wollongong, Australia. After finishing his PhD he continued his academic work with University of Kurdistan as an assistant professor. As of September 2009, he is with the Department of Telecommunication Engineering, Shiraz University of Technology, Shiraz, Iran. His research interests include data hiding, scalable image and video coding, medical image processing and biometrics.

Bahram Zahir-Azami has earned an Electrical Engineering degree from Sharif University of Technology, Tehran, a Master degree in Signal Processing from INPG, Grenoble, and a PhD degree in Communications and Electronics from ENST-Paris, obtained respectively in 1989, 1995 and 1999. He worked as a research engineer in Sharif University of Technology, Tehran, from 1989 to 1994 and later as a research assistant from 1999 to 2000 in the University of Ottawa. In January 2001 he joined Nortel Networks wireless team and worked on 3G systems (UMTS). From 2003 to 2006 Bahram worked at Hivva Technologies as chief technology officer, a startup company that he co-founded in Ottawa. He has also been a part-time professor at SITE, University of Ottawa, from 2001 to 2006. From 2007 to 2010 he has worked at the University of Kurdistan as an assistant professor. As of January 2010, he is a visiting professor at the Department of Electrical and Computer Engineering, Ryerson University, Toronto. In 2010 he established Avicenna Solutions in Toronto and works as a consultant for companies, such as Quad Infotech on scheduling optimization as of August 2010. He has published several technical papers and has one US patent. Bahram is a senior member of the IEEE.